Analyst

Integrating Nucleic Acid Sequence-Based Amplification and Microlensing for High-Sensitivity Self-Reporting Detection

Journal:	*Analyst*
Manuscript ID	AN-COM-06-2020-001231.R1
Article Type:	Communication
Date Submitted by the Author:	07-Sep-2020
Complete List of Authors:	Teng, Feiyue; Stevens Institute of Technology, Dept. of Chemical Engineering and Materials Science Wu, Xinpei; Stevens Institute of Technology, Dept. of Chemical Engineering and Materials Science Hong, Tao; Hackensack University Medical Center, Department of Pathology Munk, Gary; Hackensack University Medical Center, Clinical Virology Libera, Matthew; Stevens Institute of Technology, Dept. of Chemical Engineering and Materials Science

Integrating Nucleic Acid Sequence-Based Amplification and Microlensing for High-Sensitivity Self-Reporting Detection

Feiyue Teng,[1] Xinpei Wu,[1] Tao Hong,[2, 4] Gary B. Munk,[3, 4] and Matthew Libera[1]*

[1] Department of Chemical Engineering and Materials Science
Stevens Institute of Technology
Hoboken, New Jersey 07030, USA

[2] Microbiology & Molecular Diagnostics Laboratory
Department of Pathology
Hackensack University Medical Center
Hackensack, NJ 07601, USA

[3] Clinical Virology Laboratory
Department of Pathology
Hackensack University Medical Center
Hackensack, NJ 07601, USA

[4] Hackensack Meridian School of Medicine
at Seton Hall University
Nutley, NJ 07110, USA

Keywords: detection, microlens, microarray, microgels, molecular beacons, NASBA

ABSTRACT

We use electron-beam patterned functional microgels to integrate self-reporting molecular beacons, dielectric microlenses, and solid-phase and/or solution-phase nucleic acid amplification in a viral-detection microarray model. The detection limits for different combinations of these elements range from 10^{-10} M for direct target-beacon hybridization alone to 10^{-18} M when all elements are integrated simultaneously.

Microarray-based detection platforms offer substantial opportunities for both simplex and multiplex assays, and they continue to be developed for a range of applications.[1-3] Among these is point-of-care (PoC) diagnostics, which effectively bring a small diagnostic laboratory to the patient rather than bring patient samples to a central diagnostic laboratory.[4, 5] Challenges abound, however, because a PoC approach requires that the multicomponent process flow within a central laboratory be integrated into a single hand-held device. One component is the detection platform itself, and a microarray format is particularly attractive for PoC applications because of its simplicity and size. A specific diagnostic question - whether or not a detectable amount of target is present in a sample - can be addressed using a single array spot, and multiple array spots afford the opportunity for multiplexed diagnostics. Each spot is immobilized at a fixed position, and, for fluorescence-based PoC devices, its diagnostic question can be probed by imaging.

The efficient collection and reading of signal from the detection chip is essential to PoC devices. In the case of fluorescence-based PoC systems, their relative simplicity precludes the use of multi-element optics or bulky laser scanners to read the signal. The fixed and relatively small field of view associated with a single low-numerical-aperture (NA) lens furthermore encourages spots in an assay to be both smaller and closer together. Therefore, both locating the sensing spots and enhancing fluorescent signals are critical to the ongoing development of compact, portable, and inexpensive PoC devices.

In response, we have been exploring a materials platform for nucleic-acid diagnostics based on microgel pads electron-beam patterned onto solid surfaces from biotinylated poly(ethylene glycol) [PEG-B]. Our previous work has shown that biotinylated molecular beacon (MB) probes can be tethered to streptavidin (SA) activated PEG-B microgel pads in a format that preserves the MBs in a water-like environment with maximal degrees of conformational freedom while still preserving the surface-location specificity associated with a microarray format.[6] We subsequently have shown that amplification primers can be co-localized with the tethered MB probes,[7] and we have most recently shown that dielectric microspheres can also be tethered to the pads to provide microlensing that increases the effective NA of the collection optics.[8] Here we show that all three elements - microgel tethered MBs, self-assembled microlens, and solid-phase amplification, specifically Nucleic-Acid Sequence-Based Amplification (NASBA)[9] - can be integrated together, and we examine how different combinations of these elements influence detection limits in model simplex assays. In one combination, we achieve a limit of detection (LoD) approaching one attomolar.

A detailed description of our experimental procedure is included as Supplemental Information. Briefly, poly(ethylene glycol) [PEG] microgels are patterned from thin films (~70 nm thick) spin-cast on a silicon substrate using 2 keV electrons in a field-emission scanning electron microscope (SEM). The incident electrons locally crosslink the PEG and graft it to the underlying hard substrate. Note that the low accelerating voltage minimizes charging of the PEG film during patterning and also enables nonconductive materials such as glass to also be used as substrates. After patterning, the samples are washed thoroughly in water (developed) to remove unexposed PEG. An individual point irradiation (10 fC) creates a single microgel with a roughly gaussian thickness profile and a diameter of about 400 nm. Here we study either individual microgel spots or microgel pads with diameters ranging from 1 μm to 20 μm produced by arraying microgels at an interpixel spacing of 250 nm. Importantly, we use homopolymer PEG precursor end

functionalized with biotin [PEG-B] together with electron-irradiation conditions that preserve the biotin functionality at the surface of the microgels and microgel pads.[10] The various amplification primers, molecular beacons, and target DNA we use to functionalize and assess these patterned microgels focus on detecting influenza A virus, and their sequences are listed in Table S1 of the Supplemental Information. The details of the solid-phase NASBA process are illustrated in Figure S1 of the Supplemental Information. Bright-field and fluorescence images are collected with a Nikon E1000 upright microscope (X-cite 120 LED light source and a sCMOS Camera (pco.panda)). Fluorescence images are taken using a 40× objective (NA = 0.95) with the samples were hydrated and covered by a 0.17 mm coverslip. Fiji (ImageJ) software[11, 12] is used to analyze the digital image data.

Figure 1A illustrates the basic self-assembly elements of the detection platform. After patterning, microgels of PEG-B pads are exposed to 3 μm diameter streptavidin-functionalized polystyrene (PS) microspheres (Fig. 1A1). Biotinylated NASBA amplification primers, SP1 and SP2, then bind to SA sites on the microspheres (Fig. 1A2). We use the notation SP to designate a solid-phase primer. Finally, biotin sites on the underlying microgel pads are activated by exposure to SA, and these sites are then available to tether biotinylated molecular beacon probes. Fig. 1B shows SEM images of microspheres tethered to the biotinylated microgel pads. In the case of 1 μm diameter pads, only a single microsphere binds to each pad (Fig. 1B left). Multiple microspheres can bind to the larger microgel pads, and an average of 28 microspheres (± 2; n=36) bind to each of the 20 μm diameter pads shown on the right panel of Fig. 1B.

Figure 2 shows that microlensing substantially increases the fluorescent intensity collected from hybridized MBs. This experiment involves MBs tethered to individual microgels made by a single point irradiation during e-beam patterning and subsequently exposed to synthetic (+)DNA target (see Supplemental Information). While there is observable intensity from seven distinct microgels with no microsphere (Fig. 2A left), the intensity is clearly much higher when microspheres are involved (Fig. 2A right). The microspheres provide a lensing action that focuses a broader angular range of light emitted from the underlying MBs into the objective lens of the microscope, thus effectively increasing the numerical aperture of that objective. This lensing effect is well known.[13-17] The titration curves given in Figure 2B, generated by exposing the microgel-tethered MBs to complimentary DNA, more quantitatively illustrate the effect of the lensing. At the high concentrations, 10^{-8} to 10^{-6} M, the lensing action increases the signal intensity by a factor of about 10 (intensity with microlens/intensity without microlens), which is consistent with similar experiments we have recently done.[8] While more detailed approaches have been described,[18] we define the limit of detection (LoD) by the target concentration that produces a signal exceeding the background intensity plus five times the square root of that intensity,[7, 19] and we find that the limit of detection with and without microlenses is 1.5×10^{-10} M and 1.8×10^{-10} M, respectively (Fig. 2B inset). That these LoDs are similar can be attributed to the fact that, in addition to enhancing the collection of the fluorescent signal from hybridized MBs, microlensing also enhances collection of the background intensity produced by insufficiently quenched MB hairpins. Hence, by themselves, the self-assembled microlenses do not necessarily enhance assay sensitivity. They do, however, dramatically strengthen the overall fluorescent signal collected as well as create overall larger feature sizes, both of which lend themselves well to potential translation to a PoC-based detection system with simple optics.

We study three different configurations incorporating NASBA into a platform that combines microlensing with microgel-tethered MBs. One, solid-phase NASBA (SP NASBA) involves only solid-phase primers, where biotinylated primers SP1 and SP2 are grafted to SA sites on the tethered microlenses. Second, solution-phase NASBA (Soln NASBA), involves non-biotinylated primers P1 and P2 which are dispersed in the reaction buffer. The third combines both solution-phase and solid-phase primers (Soln + SP NASBA). Here we test these three configurations using a model Influenza A (Flu A) simplex assay. Flu A is a negative-sense single-stranded RNA virus with an eight-fragment genome, and we first use (-)DNA to mimic one of the viral (-)RNA sequences in model titration experiments (see Supplemental Information).

A number of different reactions is possible when any of these three configurations is initiated with target (-)DNA dispersed at a controlled concentration in the buffer. The most general case is the Soln+SP NASBA where primers are both free in solution and grafted to the microlenses. These reactions are illustrated schematically by Fig. 3. The reaction begins with the hybridization of (-)DNA targets to either solution primer 1 (P1) or tethered primer (SP1). Note that the (-)DNA is not complementary to the tethered MBs and, hence, cannot hybridize to them. The hybridized primer is then extended by reverse transcriptase (RT) to form double-stranded DNA (ds-DNA) either free in solution or tethered at one end to the microlens. This process corresponds to reactions 1a and 1b, respectively, in Figs. 3A and 3B. T7 RNA polymerase then catalyzes the production of (+)RNA from the ds-DNA (Fig. 3B). A portion of the (+)RNA sequence hybridizes to tethered MBs to produce fluorescence. This process is illustrated by reaction 3 in Figs. 3C and 3D. Alternatively, the (+)RNA can bind to free P2 or tethered SP2 (reactions 2a and 2b, respectively, in Figs. 3C and 3D). The primer P2 or SP2 is then extended by RT, the (+)RNA is removed by RNase H, the (-)DNA (i.e. the extended P2 or SP2) binds to either free primer P1 or to adjacent tethered primer SP1. Then, after the extension of P1 or SP1, ds-DNA is formed as a template and transcribed by the T7 RNA polymerase. The result (Fig. 3D) is again (+)RNA formed from ds-DNA either free in solution (reaction 2a) or tethered at both ends to the microlens (reaction 2b).

Figure 4 shows that integrating solution NASBA and microlens-based solid-phase NASBA substantially increases the limit of detection. It shows titration curves after a 2 h amplification period for three cases: (i) solid-phase NASBA; (ii) solution-phase NASBA; and (iii) combined solid and solution phase NASBA. The associated limits of detection are listed within the inset table (Fig. 4). Because of variations in the total intensities, each dataset is normalized to its maximum at high (-)DNA target concentrations.

The case of solid-phase NASBA where the only amplification primers available are tethered to microlenses (Fig. 4 red curve) confirms that the NASBA reaction is operative and produces (+)RNA. There is no other source of an oligonucleotide complementary to the gel-tethered MBs. The LoD of 2.9×10^{-10} M is only slightly less than that manifested by the control experiments where gel-tethered molecular beacons are directly exposed to complementary oligonucleotide ((+)DNA target (Fig. 2)). In this latter case, (+)DNA diffusion to the tethered MBs is a limiting step. In the case of solid-phase NASBA, the (-)DNA target must also diffuse to the immobilized microlens, though because of its larger size (Table S1), its diffusivity will be lower than that of the (+)DNA. Once there, however, the (-)DNA must also hybridize to microlens-tethered P1 and then be extended (reaction 1b, Fig. 3) to form end-tethered ds-DNA before (+)RNA is produced. These

latter amplification steps are not necessary in the control experiments (Fig. 2) Importantly, the (+)RNA amplicons can either: (i) diffuse away from the microarry spot into the surrounding buffer where they are effectively removed from subsequent reaction; (2) bind to an adjacent SP2 primer, whereupon the solid-phase NASBA process is repeated (reaction pathway 2b; Fig. 3) to form ds-DNA tethered at both ends to the microlens and from which more (+)RNA is produced; or (3) bind to the tethered MBs, and it is only in this last case where fluorescent signal is generated. Hence, the fact that the LoD for solid-phase NASBA by itself is about the same or less than that of the control experiments seems reasonable.

The LoD is enhanced by five orders of magnitude in the case of solution-phase NASBA where the primers are dispersed freely in solution (Fig. 4 blue curve) rather than tethered to the microlenses. Diffusion is much less of a constraint with untethered primers. (-)DNA hybridization to P1 can occur throughout the solution. Reaction pathway 1a (Fig. 3) then creates ds-DNA in solution from which (+)RNA amplicons are produced. These can either bind directly to the tethered MBs, or they can bind to P2 in solution (reaction 2a, Fig. 3) and ultimately produce more (+)RNA in a self-amplifying cascade. The amplification process in solution can rapidly increase the average concentration of (+)RNA amplicons. In a solid-phase process where the primers are tethered to microlenses and where the amplification kinetics are somewhat different, the amplification is able to increase only the local concentration.

Combining both solution-phase and solid-phase NASBA further improves the LoD by another three orders of magnitude to 1.5×10^{-18} M (Fig. 4 green curve). In this case, all reaction pathways (Fig. 3) are possible. The solution-based primers increase the average (+)RNA concentration, and the solid-phase primers in tandem increase the local concentration. Both of these processes create self-amplifying cascades. In contrast to solid-phase amplification by itself where some fraction of the locally produced (+)RNA diffuses away from the microlens, the solution-based process produces an avalanching supply of (+)RNA in solution that reduces the driving force for (+)RNA diffusion away from the microlenses. Instead the (+)RNA is more likely to hybridize with solid-phase primers and ultimately create multiple hot spots of singly or doubly tethered ds-DNA on a microlens. In contrast to solution-based NASBA by itself, these tethered ds-DNA hotspots further increase the local concentration of (+)RNA in close proximity to the tethered MB probes. Such a two-stage (solution-phase and solid-phase) nucleic-acid amplification has been demonstrated using polymerase chain reaction (PCR) approaches, though these are ultimately limited by the supply of primers.[20, 21] Another attractive property of NASBA relative to PCR is that the net effect of NASBA is the rapid accumulation of single-stranded RNA of opposite sense to that of the original oligonucleotide target. This enables us to separately study the sensitivity of the oligonucleotide amplification reaction (Fig. 4) and molecular beacon hybridization reaction (Fig. 2) system since the targets in these two reactions are of opposite sense.

To confirm that this integrated detection platform works with viral RNA, we perform integrated assays - Soln+SP NASBA, microlensing, and self-reporting fluorescence - of three respiratory viruses relevant to public-health issues worldwide. Specifically, we test isolated viral (-)RNA from reference strains of Flu A, Flu B, and respiratory syncytial virus (RSV) (see Supplemental Information). Using a (-)RNA target rather than a (-)DNA target leads to a series of reactions much like those describe by Fig. 3, except that the hybridization of (-)RNA to P1 or SP1 (reaction pathways 1a and 1b) requires the additional steps of RNase H RNA digestion after

P1/SP1 elongation followed by P2/SP2 binding and extension. We use viral RNA isolated from Influenza A (A/Puerto Rico/8/34(H1N1)), Influenza B (B/Florida/4/2006), and respiratory syncytial virus (RSV ATCC VR-26). The experimental details are provided within the Supplemental Information. The results of three individual simplex assays together with negative controls are shown in Fig. 5. In addition to incorporating microgel-tethered molecular beacons, microlensing, and both solution-phase and solid-phase NASBA, these experiments further exploit the flexibility of electron-beam lithography to create microgel pads patterned in the shapes of A, B and R for the identification of Flu A, Flu B and RSV. While these results do not probe limits of detection, they do confirm that the assay platform is able to address clinically relevant viral RNA.

Conclusions

We demonstrate a platform for fluorescence-based microarray detection that integrates self-reporting molecular-beacon detection probes, signal-enhancing microlensing, and isothermal nucleic-acid amplification both in solution and in the solid phase. We exploit the flexible and precise patterning capabilities of electron-beam lithography to create microgel pads, not only of varying size but also of target-specific shape, from biotinylated PEG to direct the self-assembly both of streptavidin-functionalized polystyrene microspheres as well as molecular-beacon detection probes. The microspheres can act both as microlenses to enhance collection of the fluorescent signal produced by the gel-tethered molecular beacons as well as solid supports for amplification primers. Target hybridization to these tethered primers leads to the generation of ds-DNA tethered to the microspheres at one or both ends from which RNA amplicons are locally produced in an avalanching fashion. In a model simplex assay we demonstrate attomolar sensitivity. This integrative platform may be particularly significant for point-of-care diagnostic systems where small and easy-to-detect array spots can facilitate the detection process in a binary yes/no assay.

Supporting Information

The supplementary materials include:

A detailed description of the experimental procedure;
Tables S1 - S3, which provide oligonucleotide sequences for primers, probes, and targets; and
Figure S1, which illustrates the solid-phase NASBA initiation and cyclic phases.

Acknowledgement

This research project was supported by the New Jersey Health Foundation (grant #PC 51-19) and by the U.S. Army Research Office (grant # W911NF-17-1-0332).

Conflicts of interest: There are no conflicts to declare.

References

1. M. A. Campanero-Rhodes, A. Lacoma, C. Prat, E. García and D. Solís, *Analytical Chemistry*, 2020, **92**, 7437-7443.
2. A. Prasad, S. M. A. Hasan, S. Grouchy and M. R. Gartia, *The Analyst*, 2019, **144**, 197-205.
3. M. B. Miller and Y. W. Tang, *Clin Microbiol Rev*, 2009, **22**, 611-633.
4. T. R. Kozel and A. R. Burnham-Marusich, 2017, **55**, 2313-2320.
5. S. Nayak, N. R. Blumenfeld, T. Laksanasopin and S. K. Sia, *Anal Chem*, 2017, **89**, 102-123.
6. X. Dai, W. Yang, E. Firlar, S. A. E. Marras and M. Libera, *Soft Matter*, 2012, **8**, 3067-3076.
7. Y. Ma, F. Teng and M. Libera, *Analytical Chemistry*, 2018, **90**, 6532-6539.
8. F. Teng and M. Libera, *Langmuir*, 2018, **34**, 14969-14974.
9. O. L. Bodulev and I. Y. Sakharov, *Biochemistry Moscow*, 2020, **85**, 147-166.
10. X. Wu, F. Teng and M. Libera, *ACS Macro Letters*, 2019, **8**, 1252-1256.
11. C. A. Schneider, W. S. Rasband and K. W. Eliceiri, *Nature Methods*, 2012, **9**, 671.
12. J. Schindelin, I. Arganda-Carreras, E. Frise, V. Kaynig, M. Longair, T. Pietzsch, S. Preibisch, C. Rueden, S. Saalfeld, B. Schmid, J.-Y. Tinevez, D. J. White, V. Hartenstein, K. Eliceiri, P. Tomancak and A. Cardona, *Nature Methods*, 2012, **9**, 676.
13. J. P. Brody and S. R. Quake, *Applied Physics Letters*, 1999, **74**, 144-146.
14. J. J. Schwartz, S. Stavrakis and S. R. Quake, *Nature nanotechnology*, 2010, **5**, 127-132.
15. H. Yang and M. A. M. Gijs, *Analytical Chemistry*, 2013, **85**, 2064-2071.
16. H. Yang and M. A. M. Gijs, *Chem. Soc. Rev.*, 2018, **47**, 1391-1458.
17. W. Zhang and H. Lei, *Nanoscale*, 2020, **12**, 6596-6602.
18. C. A. Holstein, M. Griffin, J. Hong and P. D. Sampson, *Analytical Chemistry*, 2015, **87**, 9795-9801.
19. A. Rose, *Vison: Human and Electronic*, Plenum, New York, 1973.
20. C. Adessi, G. Matton, G. Ayala, G. Turcatti, J. J. Mermod, P. Mayer and E. Kawashima, *Nucleic Acids Research*, 2000, **28**.
21. T. Q. Hung, W. H. Chin, Y. Sun, A. Wolff and D. D. Bang, *Biosens Bioelectron*, 2017, **90**, 217-223.

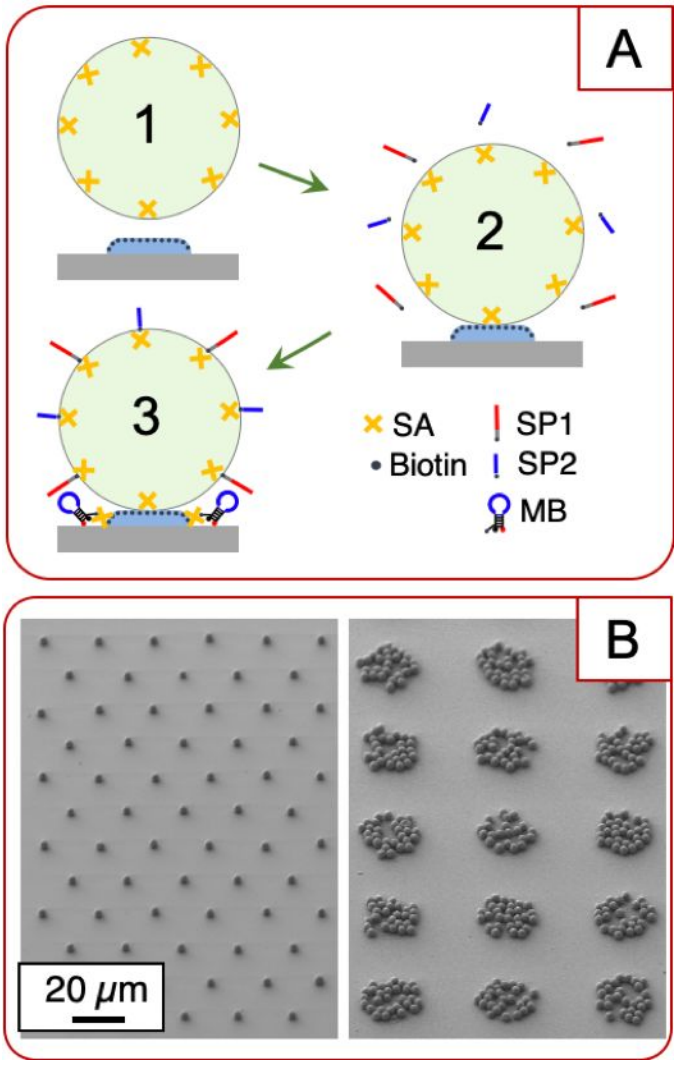

Figure 1. Nucleic-acid diagnostic array spots that integrate solid-phase amplification, microlensing, and self-reporting fluorescence. (A) Schematic illustration of the assembly process (see text); (B) SEM images of patterned microgel pads (diameter = 1 μm (left) and 20 μm (right)) showing good fidelity of microsphere self-assembly.

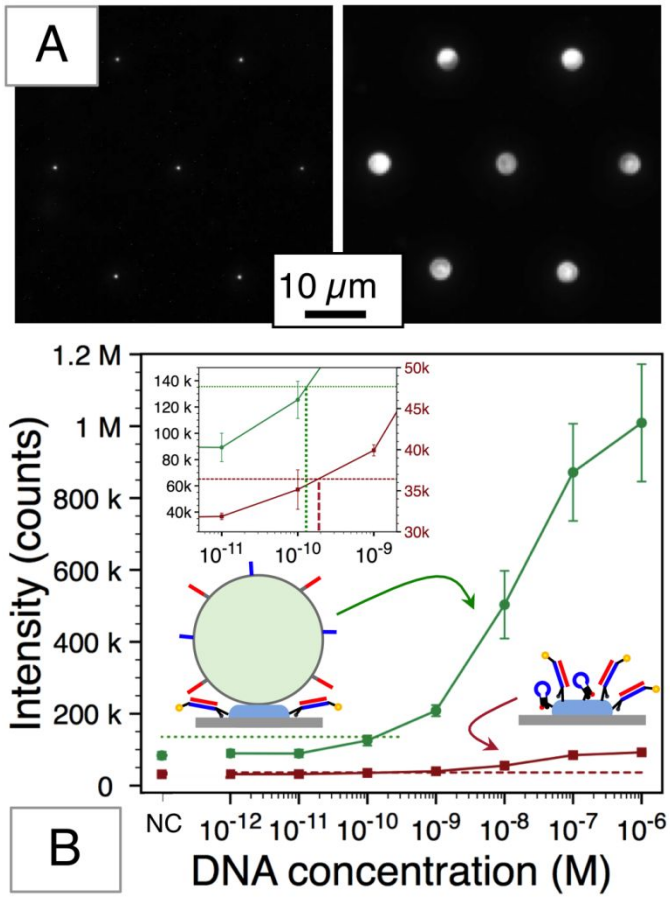

Figure 2: (A) Fluorescence images of microgel-tethered molecular beacons, without (left) and with (right) a tethered microlens, exposed to with 1 μM complementary DNA; (B) Titration curves with (green) and without (red) microlenses. The inset shows that microlensing has little effect on the limit of detection. NC represents the negative control with no target. Biotin and streptavidin molecules are omitted from this schematic.

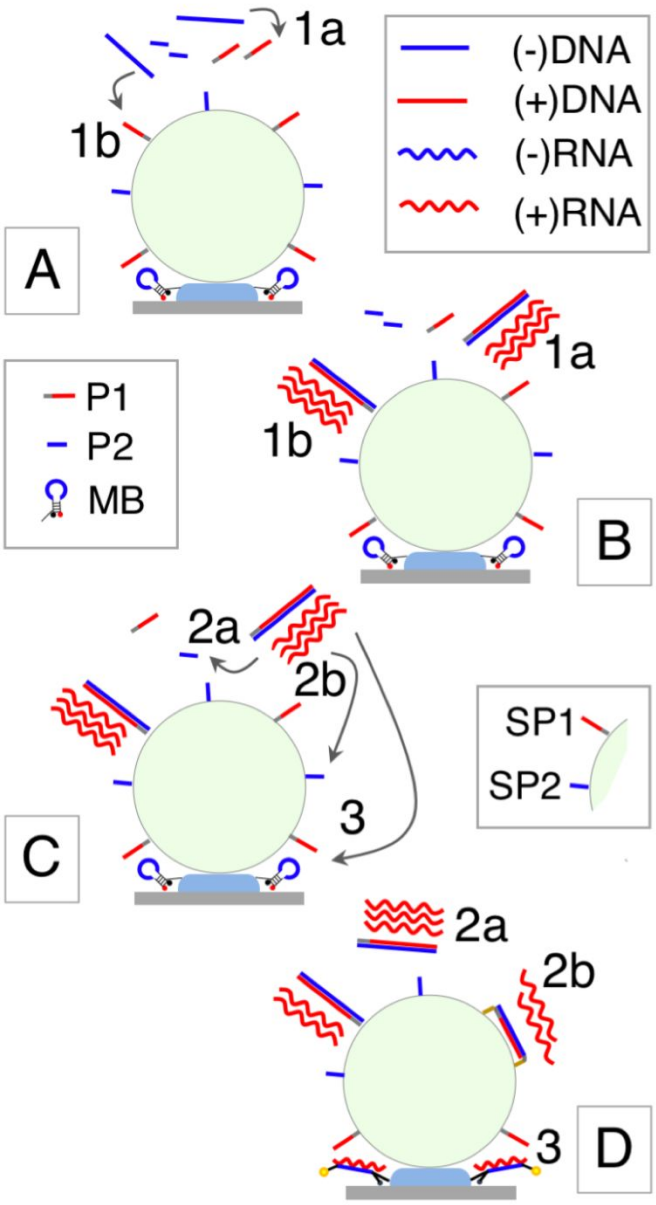

Figure 3: A schematic illustration of the various reaction pathways to produce (+)RNA amplicons from (-)DNA target in the presence of solution-phase and solid-phase primers. For solid-phase (SP) NASBA, only reaction pathway 1b and 3 can occur. For solution-phase (Soln) NASBA, only reaction pathways 1a, 2a, 3 can occur. For both (Soln+SP) NASBA, pathway 1a, 1b, 2a, 2b, and 3 can all occur. See text for a detailed description.

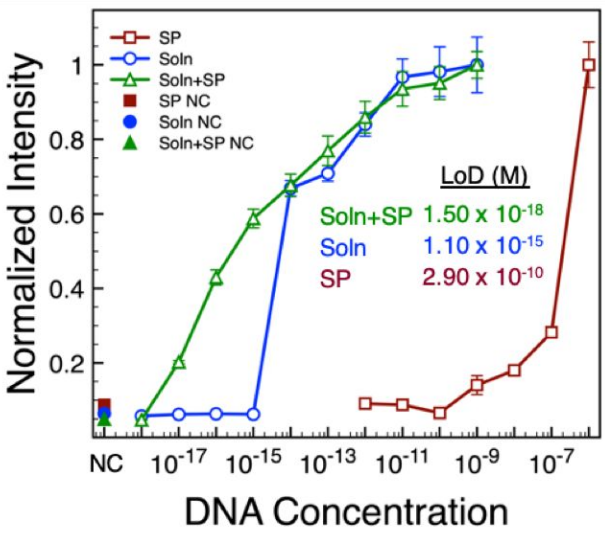

Figure 4: Titration curves for solid-phase (SP), solution-phase (Soln), and both (Soln+SP) NASBA using a (-)DNA target. The inset table gives the limits of detection (LoD) for each case. NC represents the negative control with no target.

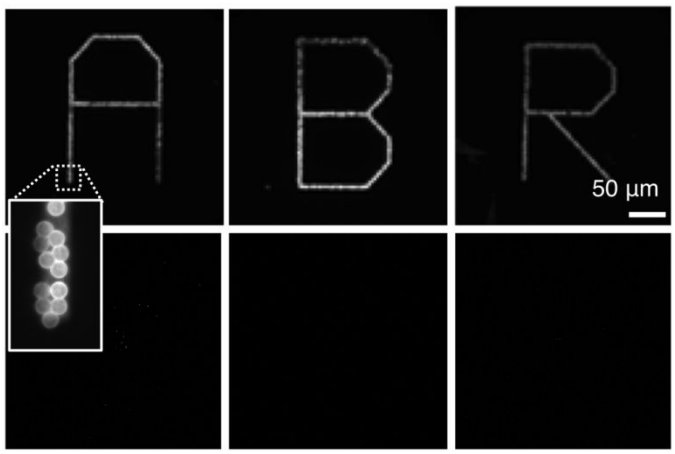

Figure 5: Fluorescence images detecting viral RNA (top row) isolated from Flu A, Flu B, and RSV with their corresponding negative control (bottom row). The inset details the microlenses tethered to the underlying patterned microgels.